1991MNRAS.250..683S

Mon. Not. R. astr. Soc. (1991) **250,** 683–691

CCD photometry of the distant young open cluster NGC 7510

Ram Sagar[1,2] and W. K. Griffiths[3]
[1]*Indian Institute of Astrophysics, Bangalore 560034, India*
[2]*Sternwarte der Universität Bonn, Auf dem Hügel 71, D-5300, Bonn 1, Germany*
[3]*Department of Physics, University of Leeds, Leeds LS2 9JT*

Accepted 1991 January 16. Received 1990 November 28; in original form 1990 July 5

SUMMARY

CCD observations in B, V and I passbands have been used to generate deep V, $(B-V)$ and V, $(V-I)$ colour–magnitude diagrams for the open cluster NGC 7510. The sample consists of 592 stars reaching down to $V=21$ mag. There appears to be non-uniform extinction over the face of the cluster with the value of colour excess, $E(B-V)$, ranging from 1.0 to 1.3 mag. The law of interstellar extinction in the direction of the cluster is found to be normal. A broad main sequence is clearly visible in both colour–magnitude diagrams. From the bluest part of the colour–magnitude diagrams, the true distance modulus to the cluster has been estimated as 12.5 ± 0.3 mag and an upper limit of 10 Myr has been assigned for the cluster age.

1 INTRODUCTION

The colour–magnitude (CM) and colour–colour (CC) diagrams of a star cluster are valuable tools for obtaining fundamental information about the cluster, such as its distance and age; for studying interstellar extinction in the direction of the cluster and for the study of stellar evolution. The distances, ages and stellar contents of young open star clusters give information on the star formation histories, structure and evolution of the galaxy. For such work, accurate observations up to $V \sim 21$ mag (6–7 magnitudes fainter than the turn-off point) are needed and they are lacking for most of the distant young open star clusters. As the introduction of modern detectors like charge-coupled devices (CCDs) make precise photometric observations possible up to that brightness with 2-m size telescopes, we observed five such clusters in 1988 July on the Isaac Newton telescope (INT) at La Palma. In the present work, observations have been presented for one of them, namely NGC 7510.

The northern galactic open cluster NGC 7510 = C2309 + 603 ($l = 110\overset{\circ}{.}96$, $b = -0\overset{\circ}{.}05$) is a member of a star complex in Cassiopeia, where star formation is still in progress (Lozinskaya, Sitnik & Lomovskii 1986). According to Lyngå (1987), it has been classified as a nebulous cluster of Trumpler class II3r. Because of its relatively large distance, the cluster has not been observed extensively. The first photometric study of the cluster was carried out by Becker, Müller & Steinlin (1955) in the RGU system. They observed 126 stars brighter than $G \sim 16.8$ mag and found only 50 of them to be possible cluster members. They derived $E(G-R) = 1.06$ mag and $E(U-G) = 0.91$ mag for the cluster reddening and 2.5 kpc as a distance to the cluster. Later on, based on *UBV* photoelectric and photographic photometry of 91 stars with a limiting magnitude $V \sim 16.1$ mag, Hoag *et al.* (1961) presented V, $(B-V)$ CM and $(U-B)$, $(B-V)$ CC diagrams for the cluster. Recently, Fenkart & Schröder (1985) carried out *UBV* photographic observations of 314 stars in the cluster region. They calibrated the observations using photoelectric data given by Hoag *et al.* (1961). They also found only 50 stars as probable cluster members. The cluster parameters derived by them are: turn-off colour, $(B-V)_0 = -0.32$ mag, earliest spectral type = O6, extinction to the cluster, $E(B-V) = 1.16$ mag, and distance to the cluster, $d = 3.14$ kpc; while in the Lyngå's (1987) catalogue, they are: $(B-V)_0 = -0.26$ mag, earliest spectral type = O9–B2, variable extinction with a mean value of $E(B-V) = 1.06$ mag, log of age = 7.0 and $d = 3.1$ kpc. The observations in lines [O II], [N II] and [S II] as well as the blue and red Palomar maps indicate that two dust shells are likely to be associated with NGC 7510 (Lozinskaya *et al.* 1986).

In this paper we describe the new *BVI* CCD photometric observations of the stars in the field of NGC 7510. These together with existing observations have been used to study the interstellar extinction across the cluster region and to estimate membership, distance and age of the cluster.

2 OBSERVATIONS

The observations were carried out in the B, V and I photometric bands, using an RCA SID 501 thinned back illuminated CCD detector at the $f/3.29$ prime focus of the 2.3-m INT at La Palma. The cluster regions were imaged only on the night of 1988 July 23–24 but observations for photoelectric standards, bias, dark- and flat-fields along with other program clusters were taken between 1988 July 21 and 23. At the prime focus, a pixel of the 320×512 size CCD corresponds to 0.74 arcsec and the entire chip covers a

© Royal Astronomical Society • Provided by the NASA Astrophysics Data System

1991MNRAS.250..683S

field of ~4.0×6.3 arcmin^2 on the sky. The read-out noise for the system was ~60 electrons pixel^{-1}, while the electrons per ADU (analogue to digital unit) was ~4. The nights were of good photometric quality with best and worst seeing ~1.2 and 2.0 arcsec, respectively. On the observing nights, the values of atmospheric extinction coefficient in the V passband determined by the Carlsberg Automatic meridian circle were between 0.10 and 0.11 mag per unit air mass with almost negligible (~ −0.003 mag) hourly rate of change of extinction. These along with mean $(B-V)$ atmospheric extinction coefficients for the site were used in determining the colour equations for the CCD system as well as zero-points for the cluster frames in the next section.

Flat-field exposures ranging from 1 to 10 s in each filter were made of the twilight sky. Altogether 11, 19 and 15 flat-field frames were taken in the passbands B, V and I, respectively. The two overlapping regions called north and south (see Plate 1) were imaged for the construction of cluster diagrams. The regions were chosen in such a way that they should cover the entire central region of the cluster, thus maximizing the number of measurable cluster members and minimizing the proportion of field stars included in the cluster diagrams. Other observing details of the cluster regions are given in Table 1. Nine Landolt (1983) standards were observed for calibration purposes. They cover a range of 10 to 12.75 mag in V and −0.19 to 1.41 mag in $(V-I)$.

3 REDUCTIONS

The data were reduced mainly at the Anglo-Australian Observatory, Epping and partly at the Astronomische Institute der Universität Bonn, Bonn using a VAX 11/780 and many μVAX computers. Initial processing of the data frames was done in the usual manner using the FIGARO data reduction package. The uniformity of the flat-fields is better than a few per cent in all filters. The averaged flat-fields were used in flat-fielding the data CCD frames.

Although the cluster fields are not exceptionally crowded, the magnitude estimation of a star on each of the frames has been done using the DAOPHOT profile-fitting software (Stetson 1987) so that it can be determined reliably to faint levels. The stellar point spread function (PSF) used by the DAOPHOT was evaluated from the sum of several uncontaminated stars present on each frame.

Further data reductions were done using the table handling facilities of STARMAN (Penny 1988). All the data frames in a colour were combined by calculating the mean frame-to-frame magnitude difference for all well-measured stars which have ~5–8 mag range in brightness. In averaging the CCD magnitudes, measures which converged with more than 50 iterations or differing from the mean for a given star by 0.1 mag were rejected. Altogether, less than 15 per cent of the measurements were rejected.

By performing synthetic aperture photometry on the photoelectric standards, the following colour equations were derived for the present CCD system:

$$\Delta I = \Delta i_{\rm CCD} + 0.012(\pm 0.007)(V-I)$$

$$\Delta V = \Delta v_{\rm CCD} - 0.006(\pm 0.006)(V-I)$$

$$\Delta B = \Delta b_{\rm CCD} + 0.109(\pm 0.008)(B-V),$$

where B, V and I are the standard mag taken from Landoldt (1983) and b, v and i with the subscript 'CCD' are the aperture mag. In converting the CCD instrumental magnitude of a star into its standard V magnitude, we applied colour corrections in terms of $(V-I)$ instead of $(B-V)$ because most of the faint stars were not detected in B. For some stars, we have measurements in B and V but not in I. The colour correction for them has been applied in terms of $(B-V)$ using the following relation:

$$\Delta V = \Delta v_{\rm CCD} - 0.009(\pm 0.005)(B-V).$$

Zero-points for the B, V and I cluster frames were determined with respect to photoelectric observations of Landolt (1983) by simply taking into account the differences in exposure times, atmospheric extinction coefficients and the difference between aperture and PSF magnitudes. The zero-points determined in this way, have an uncertainty of ~0.02 mag in B, V and I. The internal errors estimated from the scatter in the individual measures on different frames are listed in Table 2 as a function of brightness.

The X and Y pixel coordinates as well as V, $(B-V)$ and $(V-I)$ magnitudes of stars observed in NGC 7510 are listed in Table 3, along with the number of observations in each filter. Stars observed by Hoag *et al.* (1961) and Fenkart & Schröder (1985) have also been identified. Only stars with at least two measures in each filter are included in Table 3 and used in the subsequent analysis. Stars brighter than 10.5 mag on cluster CCD frames could not be measured, as they are saturated even on the short exposure frames. Stars in the magnitude range of 10.5–14.0 are generally saturated on deep exposure frames. Stars located in the overlapping area of the two cluster regions have generally been measured on 8–10 frames in each passband.

Table 1. Details of cluster observations. All the frames were taken on the night 1988 July 23–24.

Filter	North region		South region	
	Exposure time in seconds	No. of frames	Exposure time in seconds	No. of frames
B	50	4	50	4
			2	2
V	40	5	40	5
			1	2
I	60	3	30	4
	30	1	1	2

Table 2. Internal photometric errors as a function of brightness. The standard deviation (σ) is per observation in magnitudes.

Magnitude range	σ_B	σ_V	σ_I
≤ 12.0	0.005	0.009	0.012
12.0 - 14.0	0.008	0.009	0.017
14.0 - 16.0	0.010	0.014	0.019
16.0 - 17.0	0.015	0.022	0.028
17.0 - 18.0	0.021	0.041	0.032
18.0 - 19.0	0.036	0.050	0.047
19.0 - 20.0	0.053	0.053	0.055
20.0 - 21.0	0.070	0.060	0.060

© Royal Astronomical Society • Provided by the NASA Astrophysics Data System

1991MNRAS.250..683S

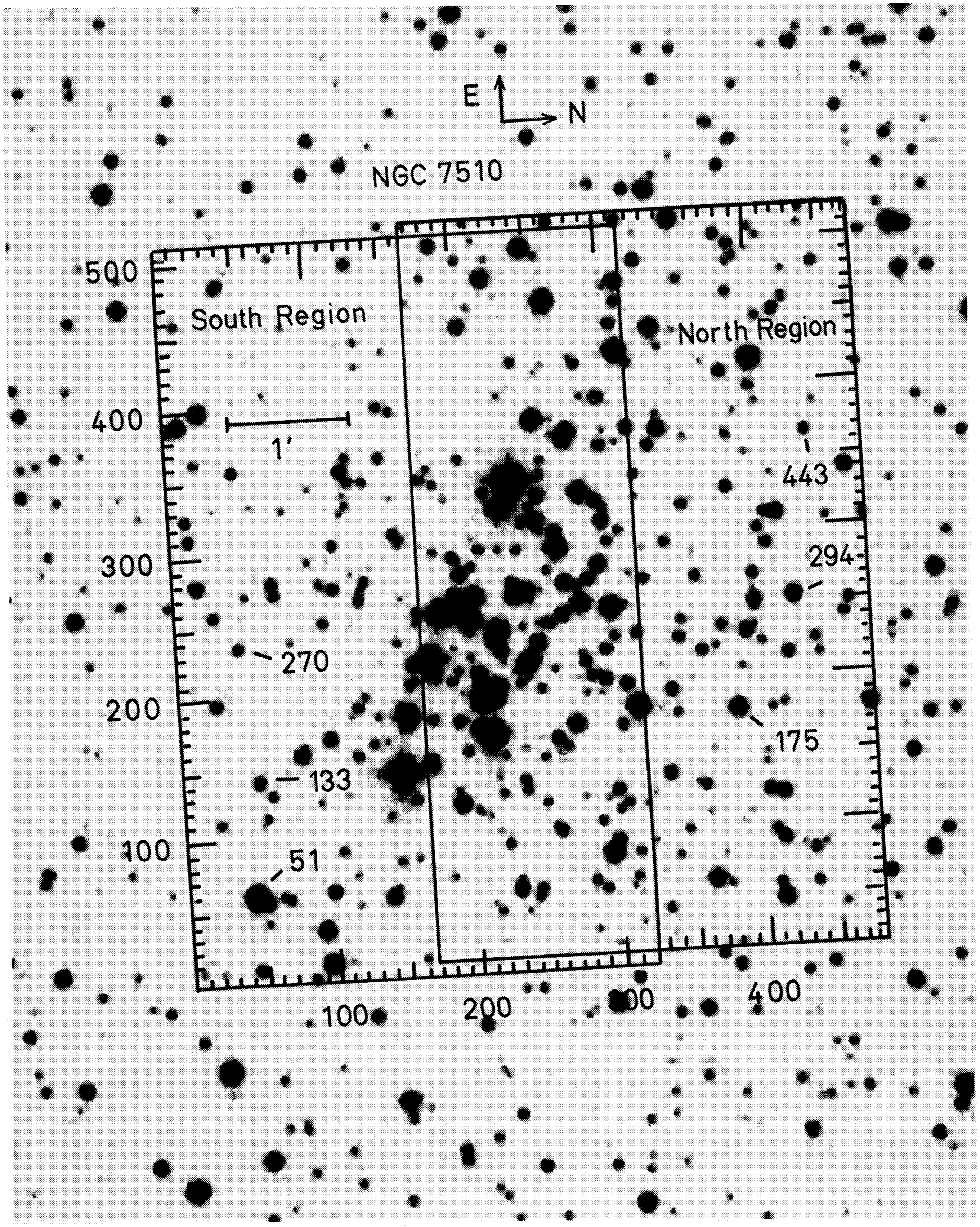

Plate 1. Identification map for the two overlapping imaged cluster regions. The map is produced from the *B* glass plate of Palomar Observatory Sky Survey and has a scale of ~2.55 arcsec mm^{-1}. North is to the right side and east is towards the top. The size of a CCD frame is ~4.0 × 6.3 arcmin^2 and the coordinates are in pixel units.

© Royal Astronomical Society • Provided by the NASA Astrophysics Data System

1991MNRAS.250..683S

© Royal Astronomical Society • Provided by the NASA Astrophysics Data System

1991MNRAS.250..683S

Table 3. Relative positions and CCD *BVI* magnitudes of stars measured in the field of NGC 7510. The numbers of observations in the *B*, *V* and *I* filters are denoted by N_b, N_v and N_i respectively. Stars observed by Fenkart & Schröder (1985) and Hoag *et al.* (1961) in the photoelectric and photographic systems have been prefixed with FS, HPE and HPG, respectively.

Star	X (pixel)	Y (pixel)	V (mag)	(B-V) (mag)	(V-I) (mag)	N_b	N_v	N_i	Other Identifications
1	130.99	10.08	20.15	-	2.61	-	4	4	
2	18.94	10.59	18.44	1.41	1.79	4	5	3	
3	4.58	10.76	17.98	1.38	1.69	4	5	4	
4	259.64	11.26	19.74	-	1.89	-	5	8	
5	45.62	11.67	15.72	0.95	1.37	3	4	3	FS58
6	162.01	13.32	17.85	1.12	1.38	4	5	4	
7	95.63	13.73	13.38	0.49	0.84	3	2	4	HPG38,FS57
8	109.77	14.37	18.64	1.47	1.95	4	4	4	
9	9.76	19.33	19.59	-	1.75	-	5	4	
10	335.04	20.29	19.25	1.62	2.07	3	3	4	
11	216.96	22.14	18.84	1.73	2.08	6	10	8	
12	452.99	23.37	18.86	-	1.78	-	3	4	
13	200.01	24.94	20.43	-	2.30	-	2	8	
14	353.85	25.23	20.53	-	2.48	-	3	4	
15	74.79	25.26	19.68	-	2.13	-	5	3	
16	159.91	25.35	19.19	1.77	2.39	3	5	4	
17	282.73	26.84	18.34	1.44	1.76	6	9	7	
18	314.83	30.12	18.74	1.31	1.64	4	10	8	
19	457.13	35.57	18.09	1.46	1.73	4	3	4	
20	92.68	37.33	14.07	0.89	1.33	3	2	4	HPE19,FS56
21	333.66	38.47	17.34	1.04	1.32	4	5	4	
22	20.51	39.16	19.77	-	2.54	-	5	4	
23	414.21	41.02	14.54	0.89	1.00	4	3	4	HPG66,FS108
24	199.07	42.27	19.86	-	1.78	-	10	8	
25	235.46	42.30	18.32	1.68	2.14	7	10	7	
26	215.81	43.10	17.58	1.24	1.55	7	10	7	
27	53.09	43.67	18.06	1.41	1.72	4	5	4	
28	286.75	48.34	20.38	-	2.10	-	4	8	
29	212.13	48.97	18.73	1.41	1.69	8	10	7	
30	316.27	50.35	19.14	1.49	1.78	4	10	4	
31	438.19	51.41	17.11	0.99	1.24	4	3	4	
32	412.02	51.73	15.76	2.35	2.72	4	3	4	FS107
33	242.65	51.93	17.09	1.20	1.52	8	10	8	
34	117.14	53.24	18.42	1.42	1.78	4	5	4	
35	377.89	53.42	18.41	0.82	1.35	4	4	4	
36	185.76	54.63	20.07	-	2.25	-	7	8	
37	290.41	54.87	17.02	1.06	1.34	8	10	8	
38	475.30	55.11	19.74	-	2.30	-	3	4	
39	281.84	55.23	19.71	-	1.95	-	7	8	
40	367.26	57.16	13.60	1.42	-	4	4	-	HPG42,FS105
41	244.93	57.53	16.54	1.05	1.31	8	10	8	FS49
42	141.29	58.17	14.74	0.93	1.26	3	5	4	HPG70,FS54
43	229.56	58.31	14.91	1.17	1.35	8	10	8	FS50
44	52.79	58.60	14.32	1.70	-	2	4	-	
45	68.56	59.75	16.82	1.27	1.60	4	5	4	
46	282.74	61.21	17.19	1.07	1.36	8	10	8	
47	312.61	61.93	17.35	1.17	1.44	8	10	8	
48	65.41	62.69	17.20	1.36	1.63	3	5	4	
49	206.97	62.96	20.08	-	2.48	-	7	8	
50	299.05	63.06	20.72	-	2.14	-	2	8	
51	45.26	63.10	11.81	1.07	1.74	2	2	2	HPG10,FS59
52	99.73	63.90	15.74	0.92	1.24	4	5	4	FS55
53	145.23	64.10	18.52	1.41	1.86	4	5	4	
54	231.18	64.52	17.61	1.32	1.73	7	10	8	
55	108.26	68.15	20.03	-	1.76	-	3	4	
56	184.47	68.72	18.08	1.43	1.64	8	10	8	
57	179.54	69.42	17.86	3.20	4.22	2	10	8	
58	169.72	70.87	20.04	-	2.04	-	8	8	
59	116.72	74.67	18.22	1.43	1.69	4	5	4	
60	437.75	74.72	16.45	1.23	1.52	4	3	4	FS110
61	374.56	74.96	18.72	1.51	1.77	4	5	4	
62	342.63	75.14	17.82	1.31	1.59	4	5	4	
63	16.14	76.75	20.12	-	2.39	-	4	4	
64	170.62	77.68	19.38	1.39	1.73	2	10	8	
65	430.03	78.26	18.77	1.38	1.65	4	3	4	
66	315.22	79.08	17.27	1.21	1.47	4	10	4	
67	444.62	79.21	18.67	1.28	1.65	3	3	4	
68	211.83	79.62	20.35	-	2.37	-	10	8	
69	295.68	79.69	13.44	0.63	1.05	8	2	6	HPG36
70	148.60	82.22	17.57	1.23	1.54	4	5	4	
71	416.53	83.24	15.94	0.90	1.11	4	3	4	FS109
72	160.60	83.58	18.14	1.24	1.55	4	5	4	
73	480.77	85.20	17.96	1.43	1.58	2	3	4	
74	326.16	86.16	18.79	1.47	1.78	3	5	4	
75	414.05	88.14	19.32	-	2.22	-	3	4	
76	300.18	88.50	15.45	1.08	1.34	8	8	8	
77	411.14	89.59	16.82	0.99	1.28	4	3	4	
78	224.48	89.83	17.10	1.20	1.55	8	10	8	
79	378.14	90.30	20.60	-	2.14	-	2	4	
80	164.59	90.41	20.38	-	2.44	-	4	4	
81	107.83	91.23	16.99	1.39	1.60	4	5	4	
82	349.91	92.88	16.51	2.23	2.58	4	5	4	FS106
83	388.65	96.76	19.29	1.38	1.90	3	5	4	
84	260.95	97.22	16.10	1.08	1.35	8	10	8	FS48
85	224.09	98.37	18.80	2.08	2.57	4	10	7	
86	12.84	99.10	20.08	-	2.29	-	5	4	
87	218.34	99.49	18.45	1.53	1.88	8	10	8	
88	258.23	101.26	18.01	1.45	1.84	8	10	8	
89	290.45	102.15	17.44	1.12	1.38	8	10	8	
90	394.82	102.80	19.04	1.34	1.68	4	5	4	
91	365.23	103.60	18.84	1.36	2.12	3	4	2	
92	303.17	109.87	17.57	1.20	1.48	7	10	8	
93	252.15	110.53	19.59	-	2.23	-	10	8	
94	212.14	110.76	18.72	1.44	1.67	8	10	7	
95	53.57	111.55	18.86	-	2.15	-	5	4	
96	321.86	112.69	18.63	1.56	2.03	3	4	4	
97	206.35	113.34	18.60	1.29	1.56	8	10	8	
98	142.77	114.12	18.05	1.31	1.72	4	5	4	
99	309.36	114.64	16.85	1.24	1.51	8	10	8	
100	24.06	114.97	17.13	1.39	1.61	4	5	4	
101	417.60	115.56	15.15	0.91	1.18	4	3	4	HPG75,FS111
102	203.88	115.94	18.14	1.35	1.69	8	10	7	
103	56.41	117.41	17.61	1.24	1.61	4	4	4	
104	385.66	117.50	19.67	-	2.35	-	5	4	
105	408.47	117.66	15.57	0.94	1.20	4	3	4	
106	252.60	118.08	17.26	1.40	1.75	8	10	8	
107	295.24	118.16	18.45	1.52	1.86	7	8	7	
108	76.88	119.30	19.06	-	1.98	-	5	4	
109	328.25	119.88	18.46	1.76	2.16	4	5	4	
110	279.26	120.57	18.43	1.55	1.88	8	10	8	
111	192.58	120.71	13.76	1.08	1.60	7	2	7	HPE16,FS11
112	388.60	121.82	20.83	-	2.30	-	2	4	
113	363.77	123.51	16.85	1.03	1.28	4	5	4	
114	302.86	124.56	16.56	0.40	1.97	5	8	5	FS47
115	161.83	124.95	17.03	1.14	1.46	4	5	4	
116	222.50	125.45	17.32	1.21	1.54	8	10	8	
117	358.57	126.02	17.85	2.45	2.82	4	5	4	
118	94.81	126.28	18.23	1.38	1.59	4	5	4	
119	239.11	127.08	16.74	1.29	1.58	8	10	8	
120	208.05	127.73	19.75	-	2.61	-	9	8	
121	191.45	130.05	18.08	1.33	1.70	7	9	7	
122	114.61	130.66	18.45	1.59	1.89	4	5	4	
123	424.13	132.27	20.49	-	2.40	-	3	4	
124	61.18	132.85	17.06	1.31	1.70	4	5	4	
125	339.24	132.86	15.56	0.97	1.23	4	5	4	HPE23,FS46
126	237.82	134.30	16.72	1.07	1.36	8	10	8	
127	407.26	136.96	18.27	1.46	1.85	4	3	4	
128	220.08	137.33	18.46	1.63	2.07	6	10	8	
129	368.19	138.79	20.93	-	2.42	-	2	4	
130	89.15	139.35	21.13	-	2.86	-	4	4	
131	220.37	140.93	18.67	1.87	2.22	2	9	8	
132	137.39	143.43	18.00	1.24	1.24	3	3	4	
133	53.06	143.91	15.57	1.32	1.63	4	5	4	FS60
134	408.38	144.92	18.25	1.57	1.72	4	3	4	
135	266.64	146.65	19.14	1.65	2.04	7	10	8	
136	231.93	147.60	20.29	-	2.29	-	2	8	
137	371.68	148.73	18.53	1.62	1.97	4	4	4	
138	253.01	149.25	17.49	1.33	1.64	8	9	8	
139	109.82	149.46	20.51	-	2.07	-	5	4	
140	71.70	149.66	19.74	-	2.45	-	5	4	
141	173.00	149.81	14.23	0.84	1.34	8	2	7	HPG59,FS10
142	432.39	150.54	20.81	-	2.55	-	2	4	
143	304.90	151.15	19.64	-	2.13	-	7	7	
144	225.39	151.67	17.82	1.39	1.62	8	9	8	
145	411.71	152.46	20.46	-	2.16	-	2	4	
146	263.37	152.66	18.06	1.90	2.31	7	10	8	
147	469.56	154.28	20.69	-	2.82	-	2	4	
148	269.81	155.60	16.87	1.61	1.94	8	10	8	
149	239.46	156.39	17.98	1.72	2.06	8	10	8	
150	198.99	156.76	16.82	1.23	1.52	8	10	8	
151	122.74	157.56	16.79	1.03	1.28	4	5	4	
152	81.20	159.77	17.35	-	1.54	-	4	4	
153	83.49	160.63	14.68	1.14	1.54	4	5	4	FS61
154	262.80	161.73	15.31	1.39	1.68	8	10	8	FS14
155	441.33	162.49	19.34	-	2.51	-	3	4	
156	251.99	163.65	18.87	1.83	2.13	2	10	8	
157	421.58	164.70	19.57	1.54	1.77	2	3	4	
158	133.84	165.29	17.26	1.12	1.33	4	5	4	
159	185.57	165.30	20.45	-	2.54	-	2	8	
160	85.71	166.45	18.61	1.22	1.64	4	4	4	
161	143.30	167.04	18.61	1.51	1.57	4	5	4	
162	216.90	167.56	10.73	0.96	1.32	2	2	2	HPG5,FS12
163	447.48	167.99	19.15	1.41	1.97	4	3	4	
164	308.32	168.42	16.73	1.14	1.39	8	10	8	
165	240.35	169.11	19.19	-	2.12	-	7	8	
166	282.62	169.23	18.88	-	2.30	-	9	7	
167	103.57	170.38	15.10	0.95	1.24	4	5	4	
168	244.06	171.07	19.79	-	1.91	-	7	8	
169	275.55	171.40	14.37	0.84	1.41	8	2	8	HPG60,FS15
170	360.47	171.79	19.04	-	3.04	-	5	4	
171	208.71	172.16	14.22	0.84	1.42	8	2	8	HPG52
172	192.68	173.13	19.14	-	1.76	-	3	7	
173	347.45	174.42	17.35	1.14	1.38	4	5	4	
174	413.44	175.52	17.34	1.54	1.84	4	3	4	
175	389.54	175.60	13.86	0.85	1.08	4	5	4	HPE18,FS112
176	193.59	177.45	16.62	1.08	1.30	8	8	8	
177	421.95	177.55	17.94	1.26	1.53	4	3	4	
178	197.45	177.91	17.46	1.17	1.42	8	8	8	
179	334.88	178.86	19.11	1.37	1.63	2	4	4	
180	375.91	179.50	20.69	-	2.54	-	3	4	
181	176.20	179.92	16.29	1.14	1.34	8	10	8	FS8
182	424.36	181.04	19.47	-	1.95	-	3	4	
183	319.90	181.26	12.33	0.89	1.11	4	5	4	HPG14,FS45
184	201.25	182.47	19.33	-	1.80	-	7	7	
185	450.13	183.84	19.91	-	2.26	-	2	4	
186	138.40	183.99	18.07	1.35	1.64	4	5	4	
187	157.78	184.06	11.99	0.80	1.13	2	2	2	HPE7,FS7
188	105.41	185.45	18.89	1.49	1.79	4	5	4	
189	119.54	185.56	18.65	1.47	1.75	4	5	4	
190	206.45	186.56	17.96	-	1.65	-	3	4	
191	210.66	189.05	13.65	0.90	1.26	8	2	4	HPG40
192	428.00	190.29	20.14	-	2.14	-	3	4	
193	343.58	190.50	15.62	1.08	1.19	4	5	4	FS44

© Royal Astronomical Society • Provided by the NASA Astrophysics Data System

1991MNRAS.250..683S

Table 3 – *continued*

Star	X (pixel)	Y (pixel)	V (mag)	(B-V) (mag)	(V-I) (mag)	N_b	N_v	N_i	Other Identifications
194	144.27	191.02	19.91	-	1.86	-	4	4	
195	124.19	191.08	16.50	1.38	1.77	4	5	4	
196	220.68	192.03	14.08	0.82	1.27	7	2	8	HPG48
197	295.48	192.08	18.47	1.64	1.96	8	10	8	
198	284.62	192.82	17.89	1.51	1.66	7	10	8	
199	204.78	193.91	17.38	1.19	1.36	5	5	7	
200	253.49	196.73	16.97	1.40	1.81	6	10	8	
201	197.78	196.86	18.58	1.65	1.91	5	6	8	
202	312.89	196.99	15.24	0.96	1.20	8	10	8	FS23
203	25.80	197.65	15.97	0.91	1.20	4	5	4	FS62
204	214.90	197.95	11.26	0.75	1.05	2	2	2	HPG7
205	129.88	198.14	16.96	1.68	2.29	4	5	4	
206	358.97	199.15	18.79	1.54	1.86	3	5	4	
207	398.67	199.30	19.39	-	2.25	-	5	4	
208	298.43	201.11	15.86	1.01	1.26	8	10	8	FS16
209	223.90	201.31	14.65	1.11	1.31	5	7	7	
210	239.31	201.47	17.16	1.09	1.36	8	10	8	
211	160.84	203.14	17.76	1.19	1.47	4	5	4	
212	280.02	203.20	18.83	1.56	1.78	2	10	8	
213	234.01	203.42	20.45	-	2.25	-	7	8	
214	289.23	203.90	16.25	1.06	1.30	8	10	8	FS17
215	138.55	204.13	20.07	-	2.55	-	4	4	
216	393.44	204.98	18.20	1.57	1.85	4	5	4	
217	191.07	205.25	17.02	1.19	1.47	8	10	8	
218	32.85	206.46	19.13	-	1.92	-	5	4	
219	294.37	206.82	18.36	2.64	2.96	2	10	7	
220	244.66	206.83	17.58	1.17	1.44	8	8	8	
221	164.97	207.27	17.17	1.10	1.34	8	5	8	
222	100.38	207.38	19.35	1.49	1.71	3	5	4	
223	252.48	208.17	19.68	-	2.05	-	7	8	
224	158.55	208.26	18.40	1.67	1.94	4	5	4	
225	181.56	208.84	17.18	1.12	1.36	7	10	8	
226	337.72	208.91	19.07	1.66	1.77	2	5	4	
227	8.40	209.43	19.45	-	1.66	-	5	4	
228	234.12	210.03	19.05	-	1.93	-	8	8	
229	209.69	210.12	14.88	0.94	1.20	8	10	8	
230	264.21	210.75	18.03	1.39	1.64	8	9	8	
231	448.60	211.53	17.84	1.21	1.48	4	3	4	
232	238.96	211.88	16.51	1.07	1.32	4	4	5	
233	195.88	212.04	17.21	1.32	1.62	8	10	8	
234	426.51	212.50	16.24	0.90	1.13	4	3	4	FS114
235	285.20	213.49	16.24	1.05	1.31	8	10	8	FS18
236	471.37	215.93	20.83	-	2.32	-	2	3	
237	227.66	216.29	18.27	1.43	1.61	6	8	8	
238	245.66	217.04	12.82	0.89	1.18	8	2	2	HPG23
239	366.34	217.09	16.49	0.95	1.18	4	5	4	FS43
240	163.95	218.58	15.78	1.02	1.28	4	5	8	
241	283.50	219.69	17.83	1.28	1.54	8	10	7	
242	376.18	220.31	17.77	1.27	1.53	4	5	4	
243	408.78	221.52	17.60	1.23	1.50	4	3	4	
244	299.54	221.62	16.12	1.02	1.29	8	10	8	FS22
245	176.12	221.69	10.72	0.87	1.21	2	2	2	HPE5,FS6
246	204.91	221.88	17.88	1.25	1.52	8	10	8	
247	446.14	222.37	16.90	1.40	1.61	4	3	4	
248	322.89	222.87	20.91	-	2.11	-	2	4	
249	140.82	222.92	19.28	-	2.00	-	5	4	
250	226.74	225.13	15.26	0.89	1.24	8	8	8	
251	210.19	225.58	19.75	-	2.38	-	6	8	
252	350.77	227.17	16.23	1.05	1.42	3	4	4	FS42
253	193.95	227.56	18.46	1.36	1.77	8	9	8	
254	386.21	228.50	19.49	-	3.05	-	3	4	
255	398.19	229.28	15.37	0.88	1.10	4	5	4	HPG86,FS113
256	252.98	229.41	14.39	0.74	1.25	8	2	8	HPG61
257	469.88	229.48	20.48	-	2.23	-	2	4	
258	306.28	230.68	17.19	1.12	1.33	8	10	8	
259	423.07	231.69	20.38	-	2.36	-	2	4	
260	222.00	232.26	14.49	0.86	1.14	8	9	6	
261	321.51	232.31	16.15	1.09	1.27	4	5	4	FS24
262	388.99	232.63	19.37	1.54	1.73	2	4	4	
263	245.55	232.64	19.92	-	2.23	-	4	6	
264	227.03	233.45	17.63	-	1.60	-	4	4	
265	282.66	233.80	20.30	-	2.11	-	7	7	
266	404.02	233.92	18.25	1.47	1.73	3	3	4	
267	381.06	234.08	16.86	1.03	1.31	4	5	4	
268	154.18	234.64	17.75	1.25	1.45	4	5	4	
269	295.31	235.11	20.77	-	2.25	-	2	7	
270	43.46	236.42	16.52	1.21	1.44	4	5	4	FS63
271	356.37	237.80	19.28	-	1.79	-	3	4	
272	467.03	239.08	16.85	1.35	1.48	4	3	4	
273	224.58	239.89	12.22	0.78	1.10	2	2	2	
274	352.13	239.92	17.12	1.29	1.57	4	5	4	
275	79.71	240.03	17.91	1.46	1.64	4	5	4	
276	242.83	240.81	17.66	1.38	1.69	7	10	8	
277	283.08	242.17	20.43	-	1.95	-	3	7	
278	261.68	242.77	16.08	0.73	1.60	6	7	4	
279	254.44	243.03	17.83	1.30	1.64	8	9	8	
280	154.95	243.88	19.59	-	1.78	-	3	4	
281	172.49	244.20	19.29	-	1.97	-	6	8	
282	360.97	246.10	19.87	-	2.28	-	4	4	
283	404.78	246.98	16.71	1.24	-	3	4	-	
284	205.81	247.41	12.17	0.78	1.08	2	2	2	HPG13
285	168.17	247.84	17.70	1.27	1.46	8	9	8	
286	271.29	248.48	14.86	0.92	1.17	8	10	8	HPG73,FS20
287	470.47	248.82	16.91	1.00	1.20	4	3	4	
288	122.80	250.18	19.47	-	2.21	-	5	4	
289	404.96	250.92	14.31	1.92	2.06	4	3	3	HPG58,FS115
290	303.99	251.17	12.70	0.77	0.96	8	2	2	HPE10,FS25
291	103.23	251.41	16.70	1.17	1.40	4	5	4	
292	315.21	252.32	18.07	1.43	1.73	4	8	3	
293	195.06	252.67	13.45	0.81	1.15	8	2	6	HPG35
294	432.41	253.19	14.57	0.89	1.04	3	2	3	HPG67,FS116
295	184.71	253.84	11.26	0.96	1.31	2	2	2	HPG8
296	169.28	254.73	16.80	1.13	1.39	8	10	8	
297	283.26	255.41	13.57	0.78	1.22	8	2	7	HPG39,FS21
298	250.36	256.22	19.55	-	1.82	-	7	8	
299	263.49	256.78	19.74	-	1.90	-	8	8	
300	200.01	257.50	19.67	-	2.28	-	2	2	
301	45.39	257.55	19.17	-	2.63	-	5	4	
302	27.24	259.17	16.07	1.52	1.86	4	5	4	FS84
303	65.43	259.51	20.02	-	2.50	-	5	4	
304	403.23	259.71	18.76	1.60	1.86	4	3	4	
305	111.27	263.04	19.70	-	2.37	-	5	4	
306	237.27	263.18	13.71	0.90	1.30	8	2	6	HPG43
307	208.64	263.66	12.81	0.78	-	2	5	-	HPG18
308	129.21	264.97	16.77	1.17	1.45	4	5	4	
309	158.17	265.17	18.56	1.46	1.80	4	5	4	
310	244.91	265.61	12.88	1.00	1.30	8	2	2	HPG22
311	195.37	265.65	15.21	0.89	1.13	8	10	8	HPG82
312	260.77	266.08	19.37	-	2.10	-	3	8	
313	256.75	266.20	18.50	1.51	1.84	6	6	8	
314	281.35	266.88	16.52	1.10	1.32	8	9	8	
315	311.81	268.80	20.24	-	2.27	-	6	8	
316	364.34	269.38	16.76	1.33	1.60	3	4	3	FS41
317	404.61	269.41	16.62	1.00	1.19	4	3	4	
318	327.87	269.69	16.77	1.00	1.23	4	5	4	
319	273.26	270.22	14.45	0.90	1.15	8	10	8	HPG64,FS27
320	332.76	271.67	19.65	-	2.15	-	3	4	
321	236.64	271.93	15.75	1.00	1.25	8	10	8	
322	290.27	272.05	15.20	1.06	1.31	8	10	8	HPG79,FS26
323	49.92	273.06	18.21	1.28	1.57	4	5	4	
324	70.44	273.70	16.03	1.32	1.49	4	5	4	
325	318.34	274.65	18.26	1.66	2.01	4	4	4	
326	213.34	275.13	19.14	-	1.80	-	9	8	
327	111.55	275.19	15.93	1.12	1.36	4	5	4	FS64
328	375.13	278.60	19.28	-	3.12	-	5	4	
329	133.29	279.16	16.60	1.18	1.44	4	5	4	
330	443.85	279.45	19.59	1.52	2.13	2	3	4	
331	324.99	279.54	20.20	-	2.27	-	3	4	
332	261.62	279.74	17.43	1.20	1.48	8	10	7	
333	200.27	279.91	14.67	0.90	1.16	8	10	8	HPG69,FS5
334	101.75	279.97	17.63	1.52	1.37	4	3	3	
335	17.13	280.53	15.07	1.01	1.19	4	5	4	FS83
336	69.00	281.15	15.81	1.25	1.63	4	5	4	
337	226.05	281.94	19.54	-	2.11	-	9	8	
338	297.63	282.05	14.48	0.84	1.56	8	2	7	HPG62,FS28
339	256.76	282.99	20.54	-	2.47	-	2	8	
340	124.63	284.83	18.67	1.54	1.94	3	5	4	
341	208.97	285.19	17.18	1.12	1.40	8	8	8	
342	363.06	287.48	18.84	1.79	2.22	2	5	4	
343	57.32	288.27	19.10	1.69	2.19	3	5	4	
344	136.84	289.11	18.65	1.69	2.02	4	5	4	
345	199.09	289.65	17.88	1.27	1.56	8	9	8	
346	415.09	289.97	16.14	1.28	1.52	4	3	4	FS117
347	328.35	291.61	18.43	1.68	1.96	3	5	4	
348	195.41	291.93	16.21	1.14	1.51	8	9	6	FS4
349	248.09	293.52	20.77	-	2.26	-	2	8	
350	253.21	293.90	19.89	-	1.97	-	4	7	
351	344.70	294.21	16.80	1.10	1.35	4	5	4	
352	109.19	294.42	18.85	1.76	2.10	4	5	4	
353	268.64	294.69	12.79	0.89	1.15	8	2	2	HPG27
354	118.38	294.88	20.24	-	2.42	-	4	4	
355	94.55	294.92	17.76	1.51	1.83	4	5	4	
356	240.97	295.12	17.10	1.19	1.54	8	10	8	
357	261.31	295.57	18.60	-	1.82	-	6	6	
358	228.30	296.25	17.75	1.24	1.51	8	10	7	
359	182.76	296.44	17.74	1.18	1.49	8	10	8	
360	214.54	296.86	16.75	0.98	1.17	8	10	8	FS3
361	304.77	297.48	16.90	1.13	1.34	7	10	8	
362	174.00	300.51	18.73	1.77	2.22	7	10	8	
363	126.43	300.75	20.47	-	2.06	-	4	4	
364	409.63	301.15	16.77	1.19	1.41	4	3	4	
365	268.90	301.94	17.53	1.11	1.45	3	4	4	
366	158.23	303.20	17.76	1.24	1.54	4	5	4	
367	313.07	304.47	17.54	1.19	1.45	8	10	7	
368	210.16	305.03	18.57	1.66	1.99	8	10	7	
369	268.22	305.37	15.10	0.93	1.18	8	10	7	HPG78
370	112.99	305.44	16.64	1.25	1.57	4	5	4	
371	162.68	306.77	18.26	1.63	2.08	4	5	4	
372	257.70	306.87	17.54	1.22	1.38	7	8	8	
373	457.83	307.08	18.14	1.36	1.64	4	3	4	
374	155.73	310.35	16.22	1.13	1.31	4	5	4	FS65
375	423.48	311.10	14.22	1.77	1.87	4	3	3	HPG56
376	301.53	311.53	15.13	0.88	1.11	8	10	8	HPG80,FS29
377	414.72	311.70	16.93	1.17	1.44	4	3	4	
378	207.47	311.77	19.77	-	2.46	-	8	8	
379	266.10	311.98	19.33	-	1.84	-	7	8	
380	13.15	313.47	16.08	1.31	1.63	4	5	4	FS82
381	245.23	313.50	16.77	1.35	1.68	8	10	8	
382	254.88	314.87	13.94	0.85	1.33	8	2	7	HPG49
383	164.33	315.92	20.53	-	2.36	-	4	4	
384	178.24	318.54	19.31	-	2.20	-	10	8	
385	435.72	319.20	20.43	-	3.11	-	2	4	
386	303.27	319.84	17.16	1.08	1.33	8	10	7	
387	358.09	320.11	16.64	1.04	1.30	4	5	4	
388	345.84	321.49	19.73	1.45	1.96	2	5	4	
389	251.51	323.89	17.12	1.18	1.37	8	9	8	
390	229.49	324.63	12.51	0.86	1.13	8	2	2	HPG17,FS2
391	364.65	325.48	19.14	1.86	2.17	2	5	4	
392	297.99	325.87	15.39	0.96	1.20	8	10	8	HPG89,FS30
393	437.42	327.03	19.41	-	3.38	-	3	4	

© Royal Astronomical Society • Provided by the NASA Astrophysics Data System

1991MNRAS.250..683S

Table 3 – *continued*

Star	X (pixel)	Y (pixel)	V (mag)	(B-V) (mag)	(V-I) (mag)	N_b	N_v	N_i	Other Identifications
394	29.19	327.30	20.11	-	2.12	-	5	4	
395	326.08	327.48	18.13	1.53	1.86	4	5	4	
396	11.48	327.58	16.66	1.09	1.46	4	5	4	
397	119.19	327.76	18.19	1.37	1.69	4	5	4	
398	337.21	329.95	20.30	-	2.16	-	2	4	
399	389.79	329.99	16.37	1.08	1.37	4	5	4	FS40
400	109.24	331.33	19.47	-	2.19	-	5	4	
401	79.16	331.55	18.05	1.37	1.71	4	5	4	
402	257.38	331.67	15.00	1.02	1.22	8	10	8	HPG76,FS32
403	286.48	333.00	13.13	0.93	-	2	8	-	HPG29,FS31
404	31.09	333.10	18.89	1.74	2.06	4	5	4	
405	123.91	333.17	17.79	1.33	1.57	4	5	4	
406	192.59	333.40	18.05	1.45	1.63	8	10	8	
407	219.81	335.26	16.56	1.05	1.21	8	10	7	
408	56.54	335.49	18.42	1.54	1.81	4	5	4	
409	154.98	335.95	18.56	1.45	1.85	4	5	4	
410	306.45	338.23	20.09	-	2.22	-	7	8	
411	420.52	338.82	18.01	1.78	2.03	4	3	4	
412	190.67	339.28	19.88	-	2.17	-	10	8	
413	122.45	340.11	18.19	1.66	1.80	4	5	3	
414	473.14	341.08	15.17	0.85	1.02	4	3	4	HPG81,FS118
415	326.26	342.69	17.06	1.00	1.25	4	5	4	
416	75.35	343.20	20.40	-	2.52	-	4	4	
417	185.13	343.42	17.33	1.12	1.41	8	10	8	
418	98.20	345.34	18.67	1.57	1.88	4	5	4	
419	260.17	346.83	17.24	1.18	1.46	6	9	8	
420	175.65	348.00	16.19	1.17	1.33	8	10	8	
421	136.53	348.11	17.18	1.27	1.48	4	5	4	
422	126.21	348.80	16.72	1.23	1.56	4	5	4	FS66
423	418.13	349.68	20.97	-	2.82	-	2	4	
424	227.83	353.46	18.48	-	0.37	-	2	7	
425	403.82	354.24	18.17	1.64	1.93	4	3	4	
426	181.87	354.51	18.00	1.32	1.61	8	10	8	
427	121.67	356.66	15.23	0.99	1.26	4	5	4	FS67
428	261.51	356.85	17.30	1.28	1.48	8	10	8	
429	46.10	360.10	16.61	1.09	1.33	4	5	4	
430	203.71	360.19	16.94	1.47	1.74	8	10	8	
431	337.03	362.47	16.32	0.96	1.16	4	5	4	FS38
432	377.86	362.74	20.40	-	2.14	-	3	4	
433	251.71	363.52	19.16	-	1.86	-	9	8	
434	303.17	364.30	16.09	0.90	1.13	7	10	8	HPG91,FS35
435	148.76	364.51	16.67	1.15	1.39	4	4	4	
436	125.59	365.73	17.00	1.19	1.54	4	5	4	
437	220.25	365.88	18.89	1.65	1.93	3	8	8	
438	177.34	365.92	19.14	-	2.23	-	10	8	
439	392.14	365.96	17.64	1.25	1.48	4	5	4	
440	314.32	366.69	18.30	1.34	1.56	4	10	8	
441	20.26	367.09	17.14	1.42	1.67	4	5	4	
442	361.95	367.21	18.16	1.46	1.78	3	5	4	
443	447.01	367.28	16.83	1.07	1.26	4	3	4	
444	278.08	368.52	15.17	0.85	1.08	8	9	7	
445	390.83	369.41	18.81	1.78	1.99	2	5	4	
446	269.67	373.25	17.86	1.50	1.71	8	10	8	
447	344.43	373.84	14.52	0.84	1.04	4	5	4	HPG65,FS39
448	280.79	375.14	13,43	0.81	0.97	8	2	7	HPG37,FS34
449	164.80	375.40	20.35	-	2.40	-	3	7	
450	305.95	375.45	18.30	1.48	1.61	8	10	8	
451	322.98	375.78	15.50	0.91	1.14	4	5	4	FS37
452	13.53	377.75	19.34	-	2.82	-	4	4	
453	294.72	378.39	20.58	-	2.33	-	2	8	
454	253.08	381.99	17.55	1.28	1.40	3	7	6	
455	398.17	382.67	18.80	1.44	1.58	3	5	4	
456	299.91	383.71	20.17	-	2.05	-	7	8	
457	474.84	384.60	20.85	-	2.09	-	2	4	
458	257.01	384.88	13.25	0.81	0.99	8	2	7	HPG32,FS33
459	344.17	384.96	17.40	1.68	2.95	4	5	4	
460	270.60	385.11	18.31	1.45	1.57	5	10	8	
461	290.63	385.70	19.64	-	1.86	-	10	8	
462	333.35	386.22	19.65	-	1.86	-	3	4	
463	209.46	386.36	21.12	-	2.12	-	2	8	
464	21.07	386.88	20.05	-	2.70	-	5	4	
465	453.61	387.82	18.15	1.51	1.68	4	3	4	
466	130.63	388.30	20.55	-	2.59	-	3	4	
467	413.32	389.60	17.88	1.47	1.63	4	3	4	
468	4.02	390.43	17.08	1.29	1.61	4	3	4	
469	310.85	393.27	19.80	-	1.71	-	8	8	
470	10.25	394.11	14.28	1.01	1.34	4	2	4	FS81
471	280.43	396.40	19.95	-	2.15	-	8	8	
472	157.88	396.49	17.37	1.18	1.45	4	4	4	
473	303.33	398.16	15.42	0.84	1.06	7	10	8	HPG87,FS36
474	291.82	400.13	18.30	1.25	1.52	8	8	8	
475	421.64	400.22	19.79	-	2.72	-	3	4	
476	410.01	400.24	16.90	1.16	1.40	4	3	4	
477	149.39	400.52	16.76	1.12	1.42	4	5	4	
478	191.58	402.49	19.85	-	2.36	-	8	8	
479	234.42	403.41	18.23	1.42	1.70	6	9	8	
480	24.84	403.96	13.48	1.18	1.30	4	2	4	FS80
481	356.55	404.25	19.53	1.57	1.78	2	5	4	
482	217.70	404.26	20.76	-	2.38	-	2	7	
483	74.26	405.96	20.78	-	2.90	-	4	4	
484	312.35	408.77	20.89	-	2.25	-	2	8	
485	242.28	409.54	19.09	1.45	1.86	8	10	8	
486	390.55	411.29	16.02	0.95	1.11	4	5	4	FS120
487	70.62	413.43	18.51	1.44	1.68	4	5	4	
488	354.94	414.75	20.90	-	2.04	-	2	2	
489	261.12	418.36	18.49	1.50	1.79	8	10	8	
490	236.41	418.37	21.06	-	2.83	-	2	8	
491	377.15	419.39	18.87	1.59	1.58	2	4	3	
492	411.25	419.57	12.77	0.81	0.98	4	3	4	HPE12,FS119
493	325.51	420.87	16.88	1.14	1.32	4	5	4	
494	289.58	422.29	16.86	1.12	1.36	6	6	7	
495	176.22	423.24	20.59	-	2.80	-	2	8	
496	266.41	423.45	17.72	2.17	2.52	8	10	7	
497	194.38	423.97	20.85	-	3.03	-	4	8	
498	245.43	425.52	16.80	1.17	1.35	7	10	7	FS69
499	215.81	426.61	20.37	-	2.14	-	4	8	
500	305.62	426.90	19.56	-	1.96	-	6	8	
501	285.97	427.20	18.46	1.29	1.55	8	10	7	
502	171.10	428.01	20.22	-	2.62	-	7	8	
503	136.21	429.92	18.11	1.51	1.73	4	5	3	
504	318.44	430.49	12.80	0.74	0.89	4	5	3	HPG28,FS122
505	348.36	431.19	17.76	1.39	1.74	4	5	4	
506	101.30	432.33	18.64	-	2.87	-	5	4	
507	425.93	435.19	20.32	-	2.39	-	3	4	
508	387.27	435.21	20.45	-	2.13	-	2	4	
509	61.04	438.06	19.28	-	2.31	-	5	4	
510	155.86	438.97	18.04	1.66	1.74	4	5	3	
511	65.73	439.45	19.43	1.43	1.83	4	5	4	
512	359.61	441.65	18.43	1.45	1.73	4	4	4	
513	52.90	441.83	18.81	-	2.51	-	5	4	
514	347.40	443.12	17.75	-	1.75	-	2	4	
515	246.44	443.15	19.68	1.56	2.20	2	10	7	
516	343.41	444.59	13.75	0.86	0.95	4	5	3	HPG46,FS121
517	123.79	445.03	18.73	1.48	1.73	3	5	4	
518	6.62	446.14	19.52	-	1.86	-	5	4	
519	136.48	446.39	17.97	1.33	1.53	3	5	3	
520	450.71	447.28	20.35	-	2.03	-	2	4	
521	180.66	448.41	20.75	-	2.35	-	3	8	
522	417.18	448.54	17.45	1.13	1.32	4	3	4	
523	315.51	448.99	16.13	0.97	1.18	4	8	4	FS123
524	429.66	452.69	16.33	0.98	1.17	4	3	4	FS134
525	209.91	453.09	15.03	0.93	1.10	8	10	8	HPG77,FS68
526	211.37	456.48	19.48	-	2.16	-	3	8	
527	193.52	457.13	20.46	-	2.12	-	2	7	
528	161.77	457.13	20.66	-	2.29	-	3	3	
529	328.30	457.18	19.34	1.69	1.64	2	3	4	
530	265.15	457.91	19.94	-	1.66	-	2	8	
531	274.30	457.94	19.58	-	1.76	-	9	6	
532	112.74	460.03	19.84	-	1.88	-	5	4	
533	86.66	460.26	17.96	1.49	1.70	4	5	3	
534	436.80	461.06	17.34	1.01	1.54	2	3	2	
535	220.45	461.64	19.40	1.55	1.97	2	10	7	
536	207.74	463.39	20.74	-	2.50	-	2	7	
537	310.70	463.51	20.81	-	2.20	-	2	4	
538	320.21	463.94	15.64	1.85	2.06	4	5	4	FS124
539	422.40	464.02	19.45	-	2.28	-	3	4	
540	11.35	464.39	17.16	1.34	1.51	4	5	4	
541	216.68	466.02	17.82	1.58	1.71	8	10	7	
542	398.05	466.13	17.23	1.07	1.31	4	5	4	
543	325.47	467.42	20.43	-	2.16	-	2	4	
544	269.99	467.46	12.68	0.77	0.86	7	2	2	HPE11,FS70
545	411.34	468.16	20.83	-	2.07	-	2	3	
546	174.71	471.39	18.33	1.34	1.65	8	10	7	
547	296.61	471.77	20.46	-	2.31	-	7	8	
548	236.01	471.83	18.21	1.57	1.79	8	10	6	
549	207.84	472.26	19.48	1.60	1.95	2	10	8	
550	25.37	472.81	20.11	-	2.36	-	5	4	
551	312.02	475.00	18.01	2.02	2.10	6	6	8	
552	364.38	477.34	17.08	1.26	1.38	4	5	4	
553	453.98	477.82	20.71	-	2.80	-	2	3	
554	321.44	478.05	14.93	0.81	0.96	3	4	4	HPG74,FS125
555	317.89	479.00	16.80	1.13	1.31	2	3	4	
556	437.52	480.73	18.20	1.47	1.47	4	3	3	
557	22.93	480.78	20.15	-	3.23	-	4	4	
558	264.86	482.41	19.41	-	1.95	-	10	8	
559	309.23	483.25	19.10	1.73	2.03	5	8	7	
560	458.87	484.29	16.85	1.27	1.38	4	3	4	
561	228.02	485.61	14.20	0.78	1.21	8	2	4	HPG57,FS73
562	240.69	486.48	18.84	1.80	2.13	4	9	6	
563	268.69	487.12	19.23	-	2.08	-	10	8	
564	368.30	487.24	20.39	-	2.04	-	3	4	
565	399.59	487.26	18.13	1.48	1.75	4	5	4	
566	186.11	487.43	17.18	1.57	1.82	8	9	8	
567	41.79	488.55	16.33	1.48	1.96	4	5	4	
568	161.35	490.87	20.00	-	2.16	-	5	4	
569	404.12	490.99	17.42	1.24	1.45	3	3	4	
570	44.15	491.51	15.82	1.64	2.13	4	5	4	FS79
571	335.13	492.21	15.66	1.11	1.20	4	5	4	FS126
572	414.63	495.50	18.75	1.53	1.76	2	3	4	
573	427.07	496.53	20.33	-	2.25	-	3	3	
574	249.30	497.04	19.92	-	1.94	-	7	8	
575	231.05	498.42	18.30	1.37	1.58	7	8	8	
576	266.51	498.44	17.67	1.35	1.60	8	10	8	
577	210.82	499.01	16.98	1.43	1.76	8	9	8	
578	187.27	499.20	19.43	1.41	1.95	2	10	7	
579	49.83	499.70	18.85	1.68	2.27	3	5	3	
580	401.58	500.16	16.23	1.16	1.20	4	5	4	FS133
581	133.38	501.58	14.45	2.85	3.27	4	2	2	FS75
582	421.16	504.53	17.37	1.71	1.93	4	3	4	
583	256.41	505.07	13.55	0.68	1.12	7	2	6	HPG41,FS72
584	392.17	506.87	16.43	1.04	1.17	4	5	4	FS132
585	181.29	507.35	20.70	-	2.31	-	2	8	
586	80.60	508.50	17.80	1.44	1.76	4	4	4	
587	193.47	509.93	15.30	1.01	1.25	8	10	8	FS74
588	335.91	510.96	18.20	1.68	1.89	4	3	4	
589	416.53	511.90	17.54	1.34	1.41	4	3	4	
590	451.09	512.27	18.28	1.26	1.50	4	3	3	
591	223.29	512.37	18.10	1.49	1.62	8	5	7	
592	166.19	517.96	18.54	1.56	-	5	4	-	

© Royal Astronomical Society • Provided by the NASA Astrophysics Data System

1991MNRAS.250..683S

To compare the present photometry with that of Hoag *et al.* (1961) and Fenkart & Schröder (1985), the differences in the sense CCD minus the other data are plotted in Fig. 1 and the statistical results are listed in Table 4. These show that:

(i) The *BV* photoelectric data of Hoag *et al.* (1961) are in good agreement with the CCD data.

(ii) For stars located in uncrowded regions, the *BV* photographic data of Hoag *et al.* (1961) and Fenkart & Schröder (1985) show no systematic difference with the CCD data. The statistical results for photographic data are based on such stars, by excluding a few points discrepant by more than 3.5 σ.

(iii) In crowded regions, photographic measures are generally brighter than the CCD measures. The errors are more likely to lie in the photographic observations given the superior performance of the CCD as a photometer and the techniques used in data reduction.

4 INTERSTELLAR EXTINCTION IN THE DIRECTION OF CLUSTER

In order to estimate interstellar extinction to the cluster, we used the $(U-B)$ versus $(B-V)$ diagram constructed from the data given by Hoag *et al.* (1961) and Fenkart & Schröder (1985). By fitting the intrinsic zero-age main sequence (ZAMS) given by Schmidt-Kaler (1982) to the cluster main sequence (MS), we find that for MS stars, the value of $E(B-V)$ varies from 1.0 to 1.3 mag. The dispersion in the $E(B-V)$ values cannot be due only to errors in the photographic data because the more precise photoelectric data also show a similar amount of scatter. This indicates that non-uniform interstellar extinction is present across the cluster region and matter present between the cluster and Earth causes a minimum extinction of $E(B-V)=1.0$ mag. The presence of non-uniform extinction in the cluster region has also been indicated by Lyngå (1987) without quantifying it. Non-uniform extinction could be due to the two dust shells associated with NGC 7510 (Lozinskaya *et al.* 1986).

The present data in combination with the *UBV* photoelectric data of Hoag *et al.* (1961) have been used to determine colour excesses for early type probable cluster members listed in Table 5. The $(B-V)_0$, $E(B-V)$ amd $E(U-B)$ values have been estimated using either the spectral type (available only for stars 3, 5 and 7 from Mermilliod 1986) or the *UBV* photometric Q method (*cf.* Johnson & Morgan 1953; Sagar & Joshi 1979) and the calibrations given by Schmidt-Kaler (1982). The $E(V-I)$ value has been estimated using Walker's (1985) calibration between $(B-V)_0$ and $(V-I)_0$, and the present $(V-I)$ measurements. For a normal interstellar extinction law, the ratio $E(U-B)/E(B-V)=0.72$ (Schmidt-Kaler 1982) and $E(V-I)/E(B-V)=1.25$ (Dean, Warren & Cousins 1978). The mean values of $E(U-B)/E(B-V)$ and $E(V-I)/E(B-V)$ (see Table

Table 4. Statistical results of the photometric comparison. The difference is always in the sense present minus comparison data. The mean and standard deviation (σ) are based on N stars. In comparison with photographic data, only stars located in uncrowded regions have been used. A few points discrepant by more than 3.5 σ have been excluded from the analysis.

Comparison data	Difference in V			Difference in (B-V)		
	Mean	σ	N	Mean	σ	N
Hoag *et al.* (1961) photoelectric	0.014	0.040	9	-0.012	0.047	9
Hoag *et al.* (1961) photographic	0.036	0.059	40	-0.038	0.064	38
Fenkart & Schröder (1985) photographic	0.043	0.115	55	-0.010	0.094	61

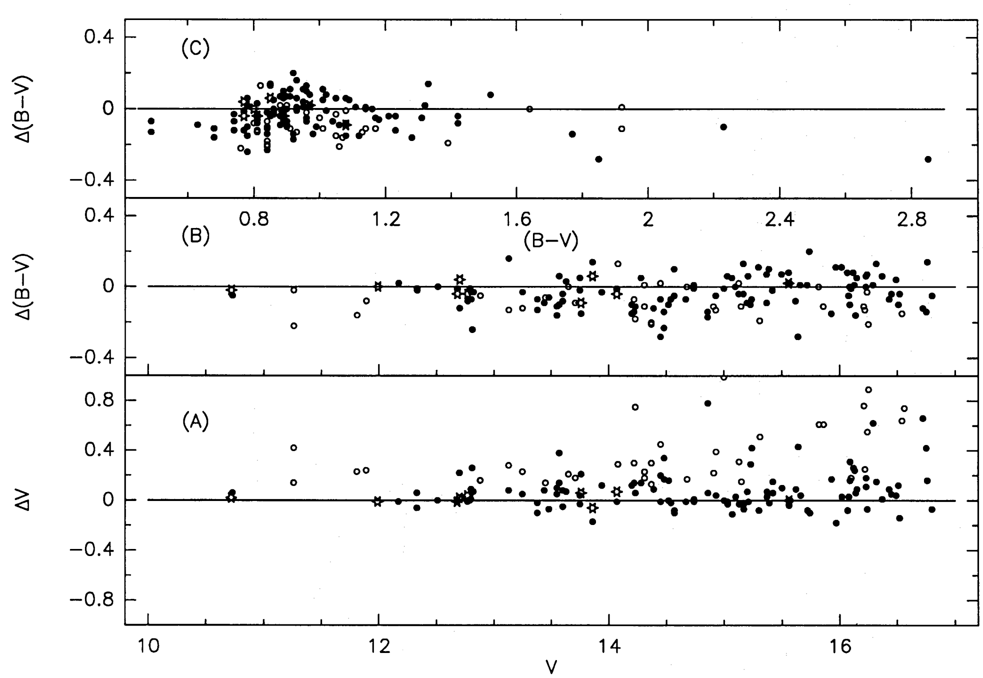

Figure 1. A comparison of the present photometry with data given by Hoag *et al.* (1961) and Fenkart & Schröder (1985). The differences (Δ) are in the sense present minus others' data, plotted against the CCD photometry. Asterisks denote Hoag *et al.*'s (1961) photoelectric data while open and filled circles represent photographic data in crowded and uncrowded regions respectively.

© Royal Astronomical Society • Provided by the NASA Astrophysics Data System

1991MNRAS.250..683S

5) are in good agreement with the normal values. Consequently, we assume that the law of interstellar extinction in the direction of the cluster is normal.

5 COLOUR-MAGNITUDE DIAGRAMS AND FIELD STAR CONTAMINATION

We have plotted V, $(B-V)$ and V, $(V-I)$ CM diagrams for all the measured stars in Fig. 2(a) and (b), respectively. Stars observed photoelectrically by Hoag *et al.* (1961) but not present in our sample have also been plotted in Fig. 2(a). It is difficult to separate field stars from the cluster members only on the basis of their closeness to the main populated area of the CM diagrams because field stars at cluster distance and reddening will also occupy this area. However, the possibility of cluster membership is small for the stars located well away from the MS, shown by open circles in Fig. 2. To know the actual number of cluster members from the remaining stars, their precise proper motion and/or radial velocity measurements are required. However, it is unlikely that all the stars fainter than $V \sim 16$ mag are field stars as indicated by Fenkart & Schröder (1985) on the basis of V, $(U-B)$ diagram of the cluster region.

A broad but well-defined cluster MS is clearly visible in the magnitude range of $13 \leq V \leq 19$. The effects of stellar evolution are not visible in the CM diagrams. To quantify the intrinsic width of observed MS, we have carried out the following simple analysis. The stars located between the eye defined blue and red envelopes of the MS have been binned in V. The colour difference (Δ) between the envelopes along with the dispersion σ_0 as a function of V magnitude has been given in Table 6. Although, the total photometric error present in our measurements is at least a combination of (a) the measuring error in each frame (internal error), (b) the intrinsic error involved in the standard stars used for calibration and (c) the uncertainties in the transformations to the standard system; the scatter, σ_E, expected in $(B-V)$ and $(V-I)$ at any given V, will arise purely from (a). The value of such scatter has been estimated from Table 2 and the results are listed in Table 6. Assuming Gaussian distributions for σ_O and σ_E, the intrinsic widths σ_I of the MS in $(B-V)$ and $(V-I)$, are estimated as $\sigma_I^2 = \sigma_O^2 - \sigma_E^2$. The intrinsic width, σ_I in $(V-I)$ is generally greater than in $(B-V)$. Most probably, presence of variable interstellar extinction across the cluster region is responsible for this because $E(V-I) = 1.25\ E(B-V)$. As a statistically significant difference exists between σ_O and σ_E for $V \leq 18$ mag, the estimates of σ_I should be considered reliable down to this limit.

The above analysis clearly indicates the presence of intrinsic dispersion in the observed MS. In addition to the presence of variable extinction across the cluster region, other main sources responsible for such dispersion can be the presence of field stars, binaries, variables and peculiars in the sample. It is not possible to assess from our observations

Table 5. Intrinsic $(B-V)$, $E(B-V)$ and colour excess ratios for probable cluster members with photoelectric $(U-B)$ observations. Star numbers are from the photoelectric list of Hoag *et al.* (1961).

Star	$(B-V)_o$	E(B-V)	E(U-B)/ E(B-V)	E(V-I)/ E(B-V)
3	-0.25	1.09	0.66	-
5	-0.28	1.15	0.68	1.31
7	-0.21	1.01	0.46	1.33
10	-0.29	1.06	0.75	1.20
11	-0.31	1.08	0.71	1.11
12	-0.20	1.01	0.73	1.17
16	-0.21	1.29	0.73	1.40
17	-0.27	1.18	0.74	-
18	-0.24	1.09	0.72	1.22
19	-0.22	1.11	0.72	1.40
20	-0.23	1.11	0.71	-
21	-0.19	1.30	0.73	-
22	-0.14	1.07	0.70	-
23	-0.20	1.17	0.74	1.22
Mean $\pm\sigma$	-0.23 $\pm$ 0.05	1.12 $\pm$ 0.09	0.72 $\pm$ 0.03	1.26 $\pm$ 0.10

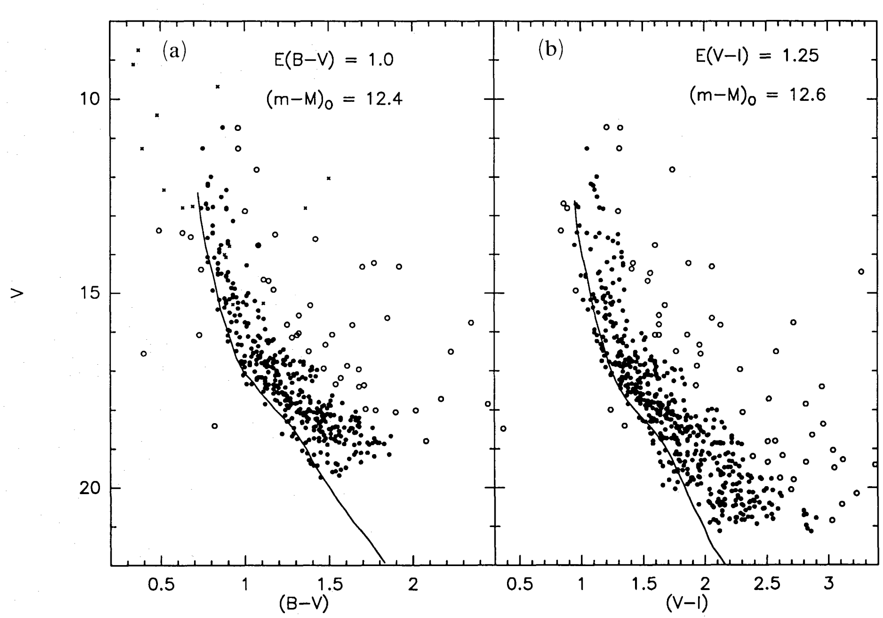

Figure 2. (a) V, $(B-V)$ and (b) V, $(V-I)$ diagrams for all the measured stars in NGC 7510. Crosses denote the stars observed photoelectrically but not present in our sample. The proposed non-members are shown as open circles.

© Royal Astronomical Society • Provided by the NASA Astrophysics Data System

1991MNRAS.250..683S

Table 6. Width of the main sequence of NGC 7510.

Range in V (mag)	Δ(B-V) (mag)	N	σ_O (mag)	σ_E (mag)	σ_I (mag)	Δ(V-I) (mag)	N	σ_O (mag)	σ_E (mag)	σ_I (mag)
	Dispersion in (B-V)					Dispersion in (V-I)				
12-14	0.17	21	0.053	0.012	0.052	0.27	23	0.134	0.019	0.133
14-16	0.22	52	0.089	0.017	0.087	0.30	50	0.096	0.024	0.093
16-17	0.31	75	0.122	0.027	0.119	0.36	72	0.130	0.036	0.125
17-18	0.37	95	0.133	0.046	0.125	0.42	99	0.137	0.052	0.127
18-19	0.40	110	0.149	0.062	0.136	0.53	113	0.190	0.069	0.177

the contribution that each of these factors contribute to the spread in colour.

As most of the factors responsible for the colour spread in the MS will redden the stars, we have used the blue envelope of the MS in CM diagrams for the estimation of distance and of age of the cluster. In this process, the colour spread expected from the observational error has been taken into account.

6 DISTANCE TO THE CLUSTER

In order to estimate the distance modulus of NGC 7510, we have used the Pleiades sequence given by Walker (1985). The sequence has been converted into the observational plane using the minimum value of $E(B-V)=1.0$ mag for a star of $(B-V)_0=0.0$ mag and the following relations for the estimation of $E(B-V)$ and $E(V-I)$ (Dean *et al.* 1978)

$$E(B-V)=1.0[1.0-0.08(B-V)_0]$$

and

$$E(V-I)=1.25E(B-V)[1.0+0.06(B-V)_0+0.014E(B-V)].$$

For the ratio of total to selective absorption we have adopted the expression given by Walker (1987)

$$R=A_v/E(B-V)=3.06+0.25(B-V)_0+0.05E(B-V).$$

After accounting for the colour dispersion expected from the error in the observations, the visual fit of the ZAMS to the bluest envelope of the CM diagrams gives $(m-M)_0=12.4$ mag from V, $(B-V)$ and 12.6 mag from V, $(V-I)$. The mean value of $(m-M)_0$ is 12.5 ± 0.3 mag where the error is estimated from the errors in R, $E(B-V)$, and the error in fitting the ZAMS. This yields a distance of 3.16 ± 0.45 kpc to the cluster, about 26 per cent greater than the estimate of Becker *et al.* (1955) but in good agreement with the values given by Fenkart & Schröder (1985) and Lyngå (1987). The present value should be considered the most reliable because it has been derived by fitting the ZAMS in a wide range (~7 mag) of the cluster MS.

7 CLUSTER AGE

As stellar evolutionary effects are not clearly visible in the CM diagrams of the cluster, an accurate estimation of the cluster age is not possible. We have estimated the cluster age by fitting the Mermilliod's (1981) empirical isochrones for NGC 6231, NGC 2362 and NGC 884 age groups to the bluest part of the V, $(B-V)$ CM diagram (Fig. 3). The isochrones have been converted from the M_v, $(B-V)_0$ plane to V, $(B-V)$ plane using the relations given in the last section and $(m-M)_0=12.5$ mag. The isochrone fitting indicates that the cluster is very young and belongs to the age group of NGC 2362.

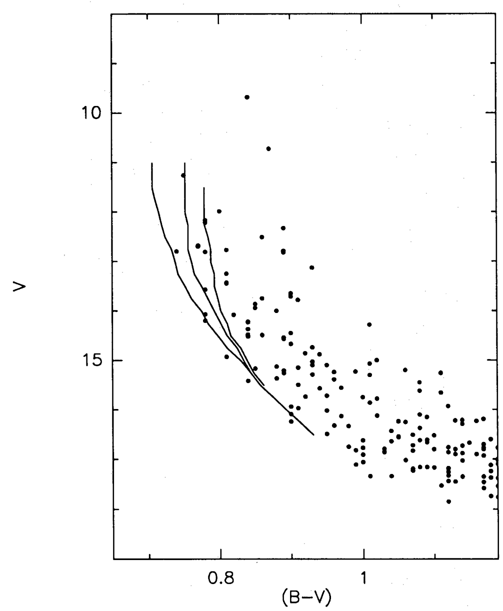

Figure 3. Fitting of the empirical isochrones to the bluest part of the V, $(B-V)$ diagram for the probable cluster member of NGC 7510. The bluest, middle and reddest isochrones are for NGC 6231, NGC 2362 and NGC 884 age group respectively.

If we consider the location of bluest star in the V, $(B-V)$ diagram as a turn-off point of the cluster, then it corresponds to $(B-V)_0=-0.28$ mag. This also indicates that cluster belongs to NGC 2362 age group (*cf.* table 7 of Mermilliod 1981). We have, therefore, assigned an upper limit of 10 Myr to the cluster age.

8 CONCLUSIONS

The new B, V and I CCD photometry down to $V=21$ mag is presented for about 600 stars in the open cluster NGC 7510. The present work leads to the following conclusions.

(i) Visual fitting of the ZAMS to the bluest envelope of the CM diagrams over a broad range of V mag (~7) gives a distance of 3.16 ± 0.45 kpc to the cluster.

(ii) Mermilliod's (1981) empirical isochrones fitted in the V $(B-V)$ diagram to probable cluster members indicate that cluster is younger than 10 Myr and belongs to the age group of NGC 2362.

(iii) In absence of kinematical data, it is difficult to separate unambiguously cluster members from the field stars only on the basis of present observations.

© Royal Astronomical Society • Provided by the NASA Astrophysics Data System

1991MNRAS.250..683S

(iv) The broad main sequence observed in the CM diagrams cannot be understood in terms of observational errors. In addition to the presence of non-uniform extinction across the cluster, the other most probable sources of MS broadening could be the presence of field stars, binaries, variables and peculiar stars in the sample.

(v) Variable reddening is present across the cluster with a minimum value of $E(B-V) \sim 1.0$ mag.

ACKNOWLEDGMENTS

The INT is operated on the island of La Palma by the Royal Greenwich Observatory in the Spanish Observatorio del Roque de los Muchachos of the Instituto de Astrofisica de Canarias. We are grateful to the PATT for the allotment of observing time and to the staff members of the La Palma Observatory for the assistance during observations. We thankfully acknowledge the comments given by Professor K. S. de Boer and the anonymous referee. We thank Professor Dr R. P. Fenkart for providing the identification map and *UBV* data before publication. One of us (RS) gratefully acknowledges the support from the Department of Industry, Technology and Commerce of Australia; the IAU and the Alexander von Humboldt Foundation. WKG is grateful to SERC for funding the observing trip.

REFERENCES

Becker, W., Müller, E. A. & Steinlin, U., 1955. *Z. Astrophys.,* **38,** 81.
Dean, F. J., Warren, P. R. & Cousins, A. W. J., 1978. *Mon. Not. R. astr. Soc.,* **183,** 569.
Fenkart, R. P. & Schröder, A., 1985. *Astr. Astrophys. Suppl.,* **59,** 83.
Hoag, A. A., Johnson, H. L., Iriarte, B., Mitchell, R. I., Hallam, K. L. & Sharples, S., 1961. *Publs US Naval Obs.,* 2nd series, Vol. 17, part 7, p. 484.
Johnson, H. L. & Morgan, W. W., 1953. *Astrophys. J.,* **117,** 313.
Landolt, A. V., 1983. *Astr. J.,* **88,** 439.
Lozinskaya, T. A., Sitnik, T. G. & Lomovskii, A. I., 1986. *Astrophys. Space Sci.,* **121,** 357.
Lyngå, G., 1987. *Catalogue of Open Cluster Data,* 5th edn, 1/1 S7041, Centre de Donnees Stellaires, Strassbourg.
Mermilliod, J.-C., 1981. *Astr. Astrophys.,* **97,** 235.
Mermilliod, J.-C., 1986. *Bull. Inform. CDS No. 31,* 175.
Penny, A. J., 1988. In: *Manual of STARMAN,* STSI, Baltimore, MD.
Schmidt-Kaler, Th., 1982. In: *Landolt/Bornstein, Numerical Data and Functional Relationship in Science and Technology,* New Series, Group VI, Vol. 2(b), p. 14, eds Schaifers, K. & Voigt, H. H., Springer-Verlag, Berlin.
Sagar, R. & Joshi, U. C., 1979. *Astrophys. Space Sci.,* **66,** 3.
Stetson, P. B., 1987. *Publs astr. Soc. Pacif.,* **99,** 191.
Walker, A. R., 1985. *Mon. Not. R. astr. Soc.,* **213,** 889.
Walker, A. R., 1987. *Mon. Not. R. astr. Soc.,* **229,** 31.

© Royal Astronomical Society • Provided by the NASA Astrophysics Data System